Biosensors and Bioelectronics 56 (2014) 64–70

Contents lists available at ScienceDirect

Biosensors and Bioelectronics

journal homepage: www.elsevier.com/locate/bios

An amperometric urea bisosensor based on covalent immobilization of urease on N_2 incorporated diamond nanowire electrode

Jayakumar Shalini [a], Kamatchi Jothiramalingam Sankaran [a], Chi-Young Lee [a,*], Nyan-Hwa Tai [a], I-Nan Lin [b,*]

[a] Department of Material Science and Engineering, National Tsing Hua University, Hsinchu 300, Taiwan, ROC
[b] Department of Physics, Tamkang University, New Taipei 251, Taiwan, ROC

ARTICLE INFO

Article history:
Received 13 September 2013
Received in revised form
21 November 2013
Accepted 28 November 2013
Available online 18 December 2013

Keywords:
N_2 incorporated diamond nanowire
Urs–GLDH/N-DNW
Urea
Cyclic voltammetry
Electrochemical impedance spectrsocopy
Amperometry

ABSTRACT

N_2 incorporated diamond nanowire (N-DNW) film electrochemical biosensor has utilized for the quantitative determination of urea in aqueous solution and urine sample. N-DNW electrode is wet-chemically cleaned (oxidation) by boiling in a mixture of H_2SO_4 and HNO_3 (3:1) at 200 °C for 2 h to remove graphite. Urease (Urs) and glutamate dehydrogenase (GLDH) are covalently attached to the oxidized N-DNW electrode by activating the COOH group of N-DNW using ethyl(dimethylaminopropyl) carbodiimide as the coupling agent and N-hydroxysuccinimide as activator. Fourier transform infrared spectroscopy and X-ray photoelectron spectroscopy data reveal that carboxylic and hydroxyl functionalized nature of N-DNW electrodes Urs–GLDH immobilized N-DNW (Urs–GLDH/N-DNW) has been successfully utilized in urea biosensor which exhibits good performance in sensitivity (6.18 μA/mg dL/cm^2), stability (~1 month), reproducibility, lower detection limit (3.87 mg/dL) and fast response time (> 10 s). Urs–GLDH/N-DNW also exhibits electrochemical response when tested for different concentration of human urine in buffer solution (from 1:9 to 4:6). In addition, Urs–GLDH/N-DNW bioelectrode retains 80% of its initial enzyme activity for < 1 month, when stored at 4–6 °C in a refrigerator.

1. Introduction

Among large number of enzymes used for biosensor construction, urease is an important part in most enzyme-based sensor development for urea detection. Urea ($(NH_2)_2CO$) is basically an organic compound made of carbon, nitrogen, oxygen and hydrogen. Most organisms deal with the excretion of nitrogen waste originating from protein and amino acid catabolism. The normal level of urea in serum is from 15 to 40 mg/dl (or 1.7–8.3 mM) and level increases up to 100 mM under pathophysiological conditions (Rick, 1990). An increase in urea level in blood and urine can be caused by renal failure, urinary tract obstruction, dehydration, shock, burns, and gastrointestinal bleeding. Moreover, reduced urea level may result in hepatic failure, nephritic syndrome, and cachexia. Determination of blood urea nitrogen is an important routine test widely used in clinical laboratories. Several types of biosensors are used for the detection and estimation of urea based on urease (Shin et al., 2008; Malhotra et al., 2008a; Renault et al., 2003). Although calorimetric and spectrometric methods are commonly used (Rosenthal, 1955; Danielsson et al., 1994), these methods are laborious and not suitable for online monitoring system. This inconvenience is overcome by using electrochemical (EC) technique. In this process, transducers transfer an electron to the electrode due to the direct conversion of a biological event to an electric signal. The inherent advantages of EC biosensors are their robustness, easy miniaturization, excellent detection limits, also with small analyte volumes and ability to be used in turbid bio-fluids with optically absorbing and fluorescing compounds (Wilson, 2005).

An important part for biosensors development is to immobilize biomolecules on the transducer without changing their structural conformation and their activity. The immobilization feature can govern the performance and reliability of the obtained biosensor. Moreover, due to the unique properties of nanostructures/nanomaterials in the biosensing area, nanosensors offer some significant advantages owing to their small size and high surface area to volume ratios allowing larger signals, better catalysis and more rapid movement of analytes through sensor (Shin et al., 2008; Malhotra et al., 2008b; Renault et al., 2003). Recently, nanostructured materials such as zinc oxide (Danielsson et al., 2011a, 2011b, 2009, 2010a, 2010b), cerium oxide (Malhotra et al., 2008c), tin oxide (Durrant et al., 2003), titanium oxide (Ju et al., 2002), iron oxide (Malhotra et al., 2008b), irconium oxide nanoparticles (Malhotra et al., 2009), layered double hydroxides (e.g. ZnAl), nanoporous alumina membranes, polymers, etc. have been used for the fabrication of transducer surface because of their unique ability to promote faster electron transfer between electrode and active site of desired enzyme. There are few reports that have shown the promising development of the third generation biosensors using such materials (Yu and Ju, 2002; Malhotra et al., 2008a; Yu et al., 2005).

* Corresponding authors.
E-mail address: cylee@mx.nthu.edu.tw (C.-Y. Lee).

0956-5663/$ - see front matter © 2013 Elsevier B.V. All rights reserved.
http://dx.doi.org/10.1016/j.bios.2013.11.071

In recent years, diamond has become an exciting material for research due to its fascinating physical properties, such as high hardness, low friction, low wear rate, chemical inertness, corrosion resistance, EC stability, high thermal conductivity, high electrical insulation, and long-term chemical stability of biomolecules bonded to it (Lin et al., 2011; Swain and Wang, 2007; Swain et al., 2005; Lin et al., 2008) makes a promising material for nano-bioelectronic devices. Precisely, diamond film electrode grown by a chemical vapor deposition process possesses enhanced EC properties with wide range of applications (Cabrera and Cunci, 2011; Davidson et al., 2008). These diamond film electrodes are synthesized by using either nitrogen or boron source, possess a high surface to volume ratio with significant π-bonding and sp^2 hybridization (Scarsbrook et al., 2002; Staryga et al., 2009; Szunerits et al., 2008) resulting in high electrical conducting behavior with distinct EC properties (Wightman and Venton, 2003). Particularly, boron doped diamond (BDD) electrodes have been widely employed for the construction of various EC biosensors due to their remarkable properties, including a wide EC potential window, low and stable capacitive background current, high response reproducibility, excellent field emission properties and good biocompatibility (Pleskov et al., 1992; Zhi et al., 2006; Fujishima et al., 1993). The functionalized or doped diamond has been used for various applications mainly in gas sensors, chemical sensors, biosensors and supercapacitors.

Recently, N_2 incorporation in growth plasma results in extreme modification in the properties of diamond materials. Incorporation of N_2 in the growth plasma leads to increase in the amorphous phase which in turn converts to a graphitic phase on annealing, defects contributing to the sp^2 at the grain boundaries, an increase in the overall grain boundary volume with increase in the density of states at Fermi level (Swain et al., 2003; Lin et al., 2010, 2012). Moreover, the EC biosensing for N_2 incorporated diamond nanowire (N-DNW) were reported in our earlier investigations for dopamine and NADH detection (Lin et al., 2013). Furthermore, low and stable capacitive background current, nontoxicity, high chemical stability and high electron transfer capability make N-DNW a promising material for sensing biomolecules involved in electron or charge transfer without need for electron mediators (Lin et al., 2013). Here, a thin film of N-DNW has been synthesized on silicon substrate by a microwave plasma enhanced chemical vapor deposition (MPECVD) technique and has been used to immobilize urease (Urs) and glutamate dehydrogenase (GLDH) using ethyl(dimethylaminopropyl) carbodiimide and N-hydroxysuccinimide (EDC–NHS) chemistry for the development of a new diamond based urea biosensor. The EC response is studied for these surface modified electrodes using cyclic voltammetry (CV) technique. The electronic structure of these N-DNW is elucidated by X-ray photoelectron spectroscopy (XPS) and Fourier transform infrared spectroscopy (FTIR) to examine the complete information about the surface chemistry of a material that altered the EC behavior of these N-DNW electrodes.

2. Experimental section

2.1. Chemicals and reagents

Chemicals were purchased at commercially available purity and were used without further treatment. Urease (Urs), glutamate dehydrogenase (GLDH), nicotinamide adenine dinucleotide (NADH), α-ketoglutarate (α-KG), N-hydroxysuccinimide (NHS), and ethyl-(dimethylaminopropyl)carbodiimide (EDC) has been purchased from Sigma-Aldrich (USA). Urs (10 mg/mL) and GLDH (1 mg/dL) solutions were freshly prepared in phosphate buffer (50 mM, pH 7.0). The stock solution of urea (100 mg/dL) was prepared in deionized water and kept at 4 °C. This stock solution is used to get different concentrations of urea by further dilution. EDC (100 mg/mL), NHS (20 mg/mL), NADH (3.7 mg/dL), and -KG (47.5 mg/dL) are freshly prepared in distilled water.

2.2. Electrode preparation

N-DNW films were grown on planar Si substrates using a MPECVD method. Prior to the deposition, the substrates were ultrasonicated in methanol solution, containing nano-diamond powder (~5.0 nm) and titanium powder (~37.0 mesh), for 45 min to create nucleation sites. The N-DNW films were grown under substrate temperature (Ts)=700 °C using 6% CH_4/94% N_2 gas at 1200 W and 120 Torr for 30 min. N-DNW electrode is wet-chemically cleaned (oxidation) by boiling in a mixture of H_2SO_4 and HNO_3 solution (3:1) at 200 °C for 2 h to remove graphite. Further Urs and GLDH were covalently attached to the N-DNW electrode by activating the COOH group of N-DNW using EDC as the coupling agent and NHS as activator (Malhotra et al., 2009). The EDC–NHS activated COOH group attached with a NH_2 terminal of Urs and GLDH results in the formation of a covalent amide bond (CO−NH). For COOH activation, the N-DNW electrode is first dipped in PBS containing 0.4 M EDC and 0.1 M NHS for 4 h at room temperature. Further, 10 μL of bienzyme solution containing Urs (10 mg/mL) and GLDH (1 mg/mL) in 1:1 ratio was immobilized by uniformly spreading on the activated electrode surface and stored for about 6 h. The Urs–GLDH/N-DNW bioelectrode is then washed with PBS buffer and is stored at 4 °C when not in use. A schematic diagram of the stepwise procedure of the bioelectrode is shown in Scheme 1.

2.3. Analytical method

The EC properties of the films were characterized using cyclic voltammetry measurements were made with CS-1087 computer-controlled potentiostat (C-V Autolab PGSTAT302, Netherlands). A standard three electrode cell was employed. N-DNW films grown using substrate temperature (Ts) 700 °C were used as working electrode (working area of 0.186 cm^2). A platinum (Pt) rod and silver/silver chloride (Ag/AgCl) electrodes served as the counter and reference electrodes respectively. Electrochemical impedance spectroscopy (EIS) measurements were performed using 1×10^{-3} mol/L $K_4Fe(CN)_6$/0.5 mol/L H_2SO_4 aqueous solution at the applied potentials of 0.196 V. All potentials in this study were reported with respect to the Ag/AgCl electrode. All measurements were made at room temperature in a 0.1 M phosphate buffer solution (PBS) with pH 7.0. De-ionized water was used throughout the experiment.

2.4. Characterization techniques

Field emission scanning electron microscopy (FESEM, JEOL JSM 6500F) was used to characterize the surface morphologies of the

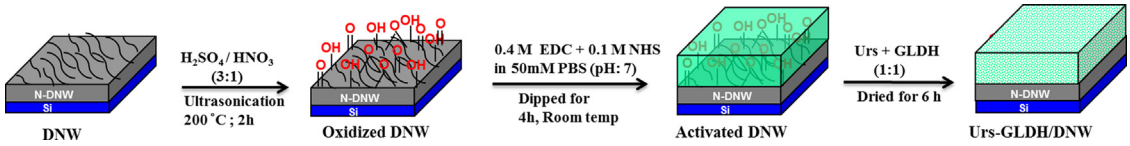

Scheme 1. Schematic representation for the preparation of biosensor.

N-DNW films. X-ray photoelectron spectroscopy (XPS) and Fourier transform infrared spectroscopy (FTIR) were used to examine the various elemental compositions that altered the EC behavior of the N-DNW electrodes. The XPS spectra of the N-DNW films obtained in this study were performed using the Al Kα-line. The measurement was conducted without ion sputtering etching, to avoid reconfiguration of the bonds.

3. Results and discussion

3.1. Materials characterization

Fig. 1a shows the FESEM image of the densely packed N-DNW films grown at Ts=700 °C in the MPECVD system possessing a characteristic 'acicular' like structure in a few nanometers width. The typical surface morphology after optimized cleaning in a mixture of H_2SO_4 and HNO_3 solution (volume fraction 3:1, 200 °C, 2 h) as shown in Fig. 1b. As seen in Fig. 1c, the FESEM micrograph of the Urs–GLDH immobilized onto activated N-DNW electrode surface exhibits covered N-DNW film surface indicating immobilization of enzyme.

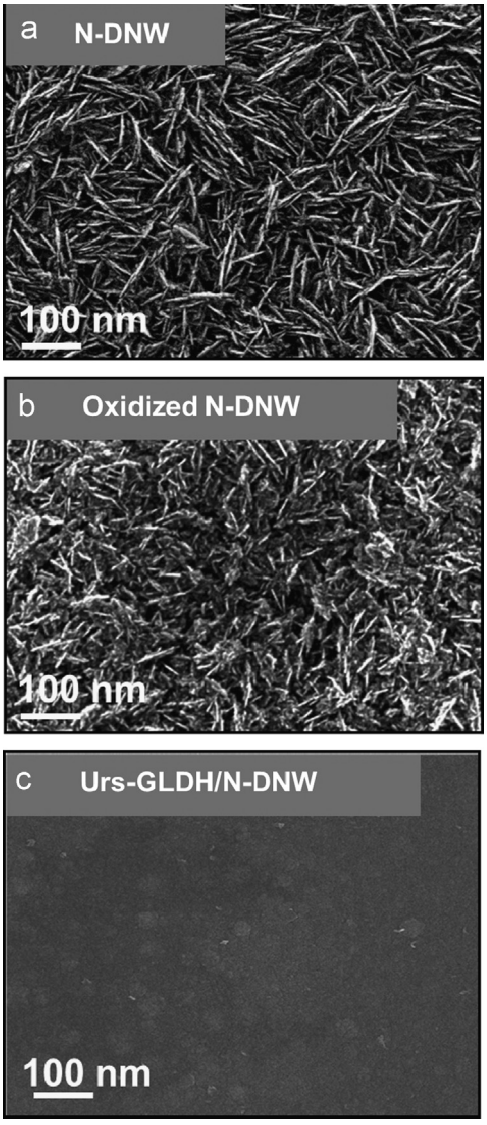

Fig. 1. FESEM micrographs during the conversion process of N-DNW into Urs–GLDH/N-DNW. It gives evidence for the conversion of N-DNW into oxidized N-DNW during acid oxidation treatment followed by covalent attachment of Urs and GLDH enzyme. (a) As grown N-DNW. (b) Oxidized N-DNW, (c) Urs–GLDH/N-DNW.

XPS is a quantitative spectroscopic technique that measures the elemental composition of a material and gives complete information about the surface chemistry of a material. Fig. 2a represents XPS studies of carbon 1s spectra of the N-DNW, oxidized N-DNW and Urs–GLDH/N-DNW respectively. It can clearly be seen that both oxidized N-DNW and Urs–GLDH/N-DNW have more C═O and C–O characteristic peak along with C═C (sp^2) peak respectively, which reflects in the hydrophilic nature of oxidized N-DNW and Urs–GLDH/N-DNW. Whereas, N-DNW observe only C═C (sp^2) characteristic peak, which exhibit the hydrophobic nature of N-DNW. In the XPS spectra, a peak obtained at 284.5 eV is attributed to the presence of a graphitic structure (sp^2, C═C). The peak obtained at 287.6 eV is assigned to the carbon 1s of the carboxylic group (C═O) for the oxidized N-DNW. A relatively large intensity peak seen at 286.3 eV for the Urs–GLDH/N-DNW is due to the presence of a C–O bond formation. Thus, XPS study confirms the formation of functionalized N-DNW.

Infrared spectroscopy is an important and popular tool for structural elucidation and compound identification. Different functional groups absorb characteristic frequencies of IR radiation. Fig. 2b shows the FTIR spectra of N-DNW, oxidized N-DNW, and Urs–GLDH/N-DNW. It is clearly observed that both oxidized N-DNW and Urs–GLDH/N-DNW have more hydrophilic functional

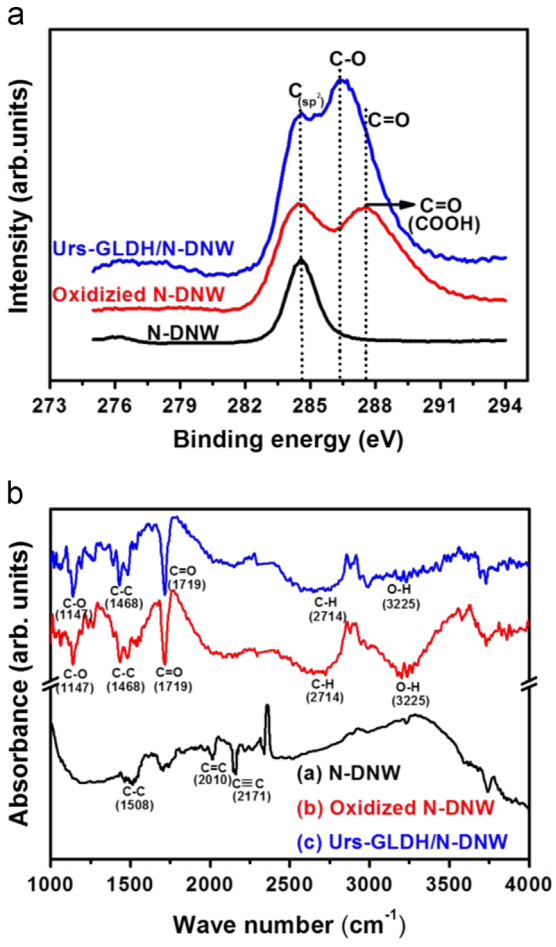

Fig. 2. (a) XPS study of N-DNW, Oxidized N-DNW and Urs–GLDH/N-DNW. In the XPS spectra, the peak at 284.5 eV is attributed to the presence of a graphitic structure (sp^2, C═C), whereas the peak at 287.6 eV is assigned to the carbon 1 s of the carboxylic group containing C═O, peak seen at 286.3 eV is due to the presence of a C–O bond for the Urs–GLDH/N-DNW. (b) FTIR spectrum of N-DNW, Oxidized N-DNW and Urs–GLDH/N-DNW. FTIR spectra reveal that both oxidized N-DNW and Urs–GLDH/N-DNW have carboxyl functional groups.

groups on the surfaces. However, none of these peaks are seen in the case of N-DNW, which exhibit the hydrophobic nature of the functional groups. The peak at 1719 cm^{-1} represents the stretching vibration of C=O bonds of the carboxylic acid group, whereas two other peaks at 2714 and 3225 cm^{-1} correspond to C–H and O–H stretching modes of the carboxylic alcohol groups, respectively. The peaks seen at 1147and 1468 cm^{-1} represent the C–O and C–C stretching modes of activated N-DNW. FTIR spectra, thus, clearly suggest that –COOH groups are present within the Urs–GLDH/N-DNW, which makes it a potential material for different applications. Therefore, both XPS and FTIR studies confirm the formation of functionalized N-DNW.

3.2. Electrochemical characterization

N-DNW, oxidized N-DNW electrode and Urs–GLDH/N-DNW bioelectrode have been characterized using the CV technique with a three-electrode system in PBS containing 5 mM $[Fe(CN)_6]^{3-/4-}$. Fig. 3a shows the CV response obtained for N-DNW, oxidized N-DNW and Urs–GLDH/N-DNW electrodes in the potential range of −0.1 to +0.5 V at a scan rate of 50 mV/s. The increase in the cathodic current obtained for the N-DNW (6.09×10^{-5} A, curve (I)) compared to oxidized N-DNW electrode (1.62×10^{-5} A, curve (II)) indicates that a larger surface area of N-DNW helps in large-scale redox conversion, resulting in an increase of redox current which reflects its enhanced electron transfer property. The decrease in the anodic current obtained for the Urs–GLDH/N-DNW electrode (3.69×10^{-5} A, curve (III)) is attributed to the hindrance caused by the macromolecular structure of enzymes indicating urease and GLDH immobilization. Fig. 3b shows the cyclic voltammogram (CV) of the Urs–GLDH/N-DNW electrode recorded at different scan rates (10–100 mV/s). It can be seen that, as we move toward a higher scan rate, anodic potential shifts more toward the positive potential and the cathodic peak potential shifts in the reverse direction. Besides this, the redox peak currents show linear behavior with the square root of the scan rate, $\nu^{1/2}$ (Fig. 3c), revealing it as a diffusion-controlled electron-transfer process. We performed EIS measurements for N-DNW, oxidized N-DNW and Urs–GLDH/N-DNW electrodes in the $Fe(CN)_6^{3-/4-}$ solution. The measured frequency range is 10^{-2}–10^{5} Hz. Fig. 3d displays a high frequency semicircle followed a low frequency straight line for N-DNW and Urs–GLDH/N-DNW electrodes. The slightly flattened semicircle at high frequency associated with the contact impedance resulted from the electrical connection between working electrode as well as that between electrode and the platinum wire. Inset in Fig. 3d shows the Randles equivalent circuit used to fit the impedance spectra. The observed semicircle in the medium frequency range for the N-DNW and Urs–GLDH/N-DNW electrode corresponds to the parallel combination of the R_{ct} and CPE_1, and the straight line corresponds to the Warburg impedance. The intercept of the semicircle with the Z' axis at high frequencies is equal to R_S, and extrapolation of the semicircle to low frequencies yields an intercept corresponding to R_S+R_{ct}. These results indicate that the N-DNW and Urs–GLDH/N-DNW electrodes exhibit facile electron transfer to the solution redox species, with $R_{ct}=1733\ \Omega$ and $1237\ \Omega$ respectively, for the $Fe(CN)_6^{-3/-4}$ redox reaction, whereas, oxidized N-DNW exhibits slightly flattened semicircle at high frequency associated with the contact impedance resulted from the electrical connection between working electrode as well as that between electrode and the platinum wire. This plot indicates fast electron transport in the bioelectrode materials

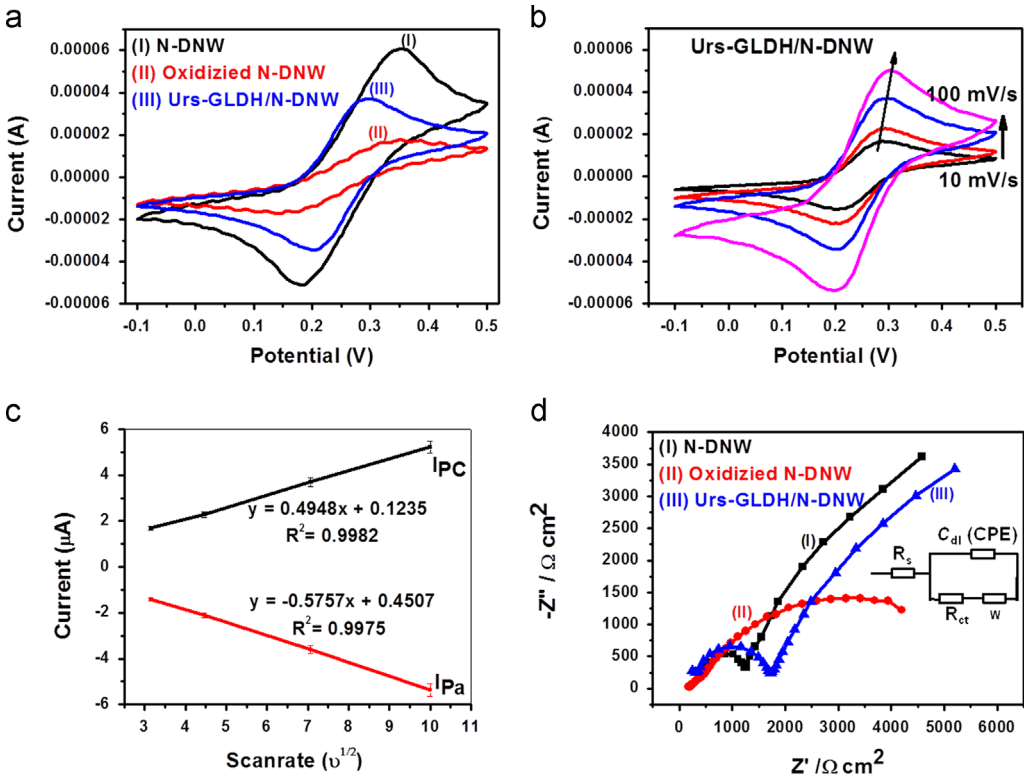

Fig. 3. (a) Cyclic voltammetry (CV) of N-DNW, Oxidized N-DNW and Urs–GLDH/N-DNW. The increase in the anodic current obtained for the N-DNW (6.09×10^{-5} A, black line) compared Oxidized N-DNW (1.62×10^{-5} A, red line) indicates that a larger surface area of N-DNW helps in large-scale redox conversion. (b) CV studies of the Urs–GLDH/N-DNW bioelectrode as a function of scan rate (10–100 mV/s). (c) Redox peak current of Urs–GLDH/N-DNW bioelectrode as a function of the square root of scan rate. This result represents that, as we move toward a higher scan rate, anodic potential shifts more toward the positive potential and the cathodic peak potential shifts in the reverse direction. (d) EIS Nyquist plot using N-DNW, oxidized N-DNW and Urs–GLDH/N-DNW film as electrochemical electrode in 0.1 M KCl containing 0.5 M $[Fe(CN_6)]^{3-/4-}$ redox couples at different potential vs. Ag/AgCl. (For interpretation of the references to color in this figure legend, the reader is referred to the web version of this article.)

and inner-sphere transfer mechanism, and the electrode kinetics is extremely sensitive to the electrode surface.

3.3. Electrochemical response towards Urs–GLDH/N-DNW bioelectrode

The effect of pH (1.0–10.0) on Urs–GLDH/N-DNW bioelectrode has been studied using CV to estimate enzyme activity that depends upon the conformation and electrostatic state of enzyme's active site. Fig. S1 (see Supporting information) shows the highest current obtained for Urs–GLDH/N-DNW bioelectrode towards 5 mM $[Fe(CN)_6]^{-3/-4}$ with pH 7 containing 20 mM urea. Therefore, pH 7 has been chosen as optimum pH for all electrocatalytic experiments.

The responses of the Urs–GLDH/N-DNW bioelectrode have been studied by the CV method as a function of urea concentration. Low and stable capacitive background current, biocompatibility, high chemical stability and high electron transfer capability make N-DNW a promising material for sensing biomolecules involved in electron or charge transfer process. During the biochemical reaction, Urs catalyzes the decomposition of urea into hydrogen bicarbonate (HCO_3^-) and ammonium (NH_4^+) ions. It has been found that ammonium ions simply diffuse into the solution. Thus it is required to add GLDH as it catalyzes the reaction among NH_4^+, α-KG, and NADH to create NAD^+ and L-glutamate. Since the Urs–GLDH enzyme were covalently attached to the N-DNW, the electrons generated during the biochemical reactions are transferred to the N-DNW electrode via an Fe(III)/Fe(IV) redox probe ensuing a signal in the form of current. The biochemical reaction is shown in Scheme 2.

The EC response studies of the Urs–GLDH/N-DNW bioelectrode obtained as a function of urea concentration in the presence of 30 μL of NADH and 70μL of α-KG in PBS solution carried out using CV technique is shown in Fig. 4a. The calibration curve was fitted between the urea concentration and the value of anodic peak current (Fig. 4b). It is found that the magnitude of the current increases linearly as urea concentration increases. The Urs–GLDH/N-DNW bioelectrode exhibits linearity as 10 – 100 mg/dL, lower detection limit of 3.87 mg/dL, with the response time of 10 s. The sensitivity of the Urs–GLDH/N-DNW bioelectrode has been estimated as 6.18 μA/mg dL/cm^2 with the regression coefficient of 0.999.

The amperometric responses of the N-DNW and Urs–GLDH/N-DNW bioelectrode to urea are depicted in Fig. 4c, showing a typical amperogram obtained by the addition of different urea concentrated analyte solutions in a stirred 0.1 M PBS (pH 7.0). We monitored the oxidation current of a specific analyte at a fixed potential of +0.2 V. The oxidation current of urea increases linearly with an increase of urea concentration for Urs–GLDH/N-DNW bioelectrode, whereas, N-DNW electrode does not show any amperometric response for the addition of different concentration of urea. The developed Urs–GLDH/N-DNW sensor was tested for diluted-urine samples for N-DNW and Urs–GLDH/N-DNW bioelectrode. Fig. 4d represents variation in the sensitivity with increasing concentration of urine in buffer solution. Urine was diluted with buffer solution from 1:9 to 4:6. Different concentrations of human urine, 0 ml, 1 ml, 2 ml, 3 ml, and 4 ml mixed with 10 ml, 9 ml, 8 ml, 7 ml, and 6 ml of PBS respectively, were further tested for urea detection, which also exhibits electrochemical response to the addition of urine in buffer solution. Increase in sensitivity is noticed with increasing urine concentration. Immobilization results in an increase in the current with applied voltage, analogous to that of urea sensing. The analytical performance indicate that detection limit, linear concentration range and sensitivity of the proposed biosensor are comparable with many urea sensors previously reported (see supporting information, Table 1) (Gemeiner et al., 2002; Kaneto et al., 2005; Do and Luo, 2004; Dong et al., 2004). The Repeatability of real time detection with different concentration of human urine in buffer solution (from 1:9 to 4:6) was carried out. We do not observe any changes in the current response.

3.4. Urs–GLDH/N-DNW bioelectrode stability

The Urs–GLDH/N-DNW electrode was also studied for the enzyme stability. The stability of the enzyme was monitored by conducting continuous measurement of the electrode current sensitivity to a 20 mM urea sample, after an interval of 2 weeks (Fig. 5a). The Urs–GLDH/N-DNW electrode remains unchanged even after exposure to the solution, followed by washing, drying, and storage in 4–6 °C in a refrigerator for 2 weeks. Moreover, the response is found to be stable for several days, even with repeated use. Very slow decrement in response current was observed to a period of 1 month. It was observed that the Urs–GLDH/N-DNW electrode retained 80% of its initial enzyme activity for <2 weeks, when stored at 4–6 °C in a refrigerator. This long-term stability of the Urs–GLDH/N-DNW electrode is comparable with the recently reported biosensors (<30 days) (Malhotra et al., 2009; Fahys et al., 2004; Walcarius et al., 2002; Kaneto et al., 2005; Do and Luo, 2004; Dong et al., 2004). Fig. 5b represents the comparative studies of Urs–GLDH immobilized N-DNW, boron doped diamond (BDD) and glassy carbon (GC) film electrodes, which clearly shows that enzyme immobilized N-DNW; BDD shows similar CV response as a function of 20 mM urea concentration in the presence of 30 μL of NADH and 70 μL of α-KG in PBS solution containing 0.5 M $[Fe(CN_6)]^{3-/4-}$ redox couples. However GC electrode shows lack in sensitivity for the urea detection due to inactivation of electrode.

4. Conclusion

This study has demonstrated the feasibility of developing a new diamond based biosensor for monitoring urea in aqueous medium.

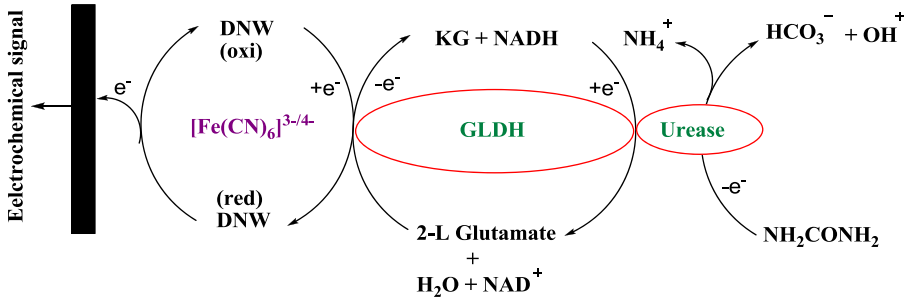

KG = Ketoglutarate
NADH = Nicotinamide adenine dinucleotide
GLDH = Glutamate dehydrogenase

Scheme 2. Possible mechanism for the biochemical reaction on bioelectrode system.

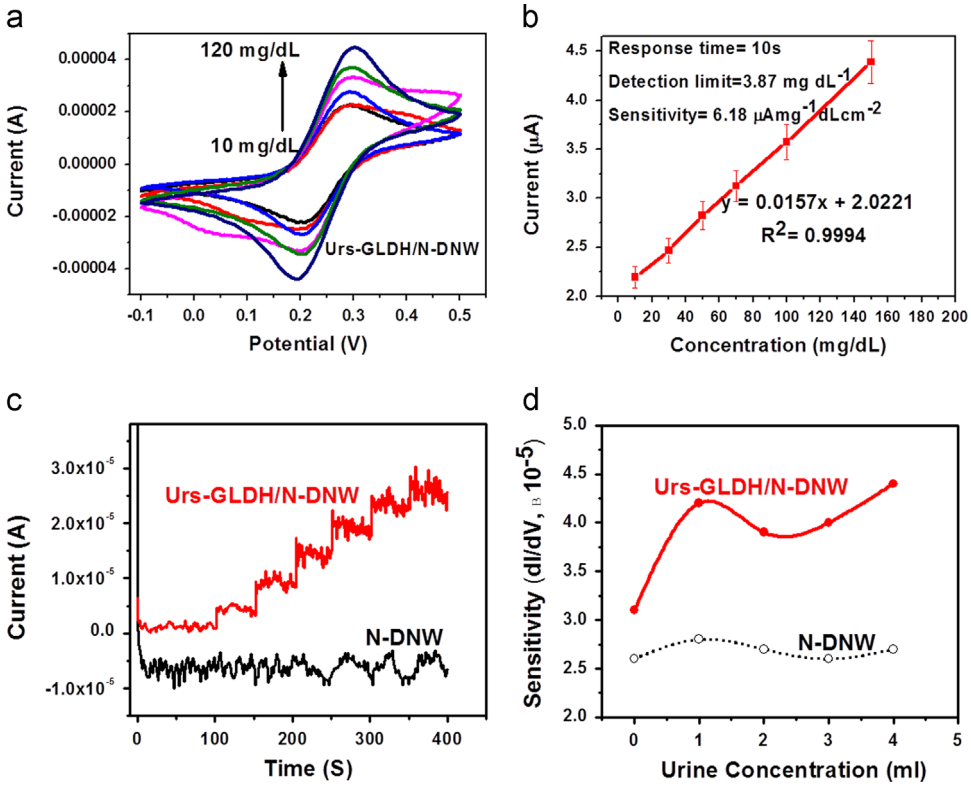

Fig. 4. (a) CV response of the Urs–GLDH/N-DNW bioelectrode as a function of urea concentration in the presence of 30 μL of NADH and 70 μL of α-KG in PBS solution. (b) Calibration curve between magnitude of the anodic peak current (I p) and urea concentration. It is found that the magnitude of the current increases linearly as urea concentration increases. (c) Amperometric responses of urea for N-DNW and Urs–GLDH/N-DNW electrodes in a 0.1 M PBS solution. (d) Sensitivity (dI/dV curves) as a function of diluted-urine concentration for the N-DNW and Urs–GLDH/N-DNW bioelectrode.

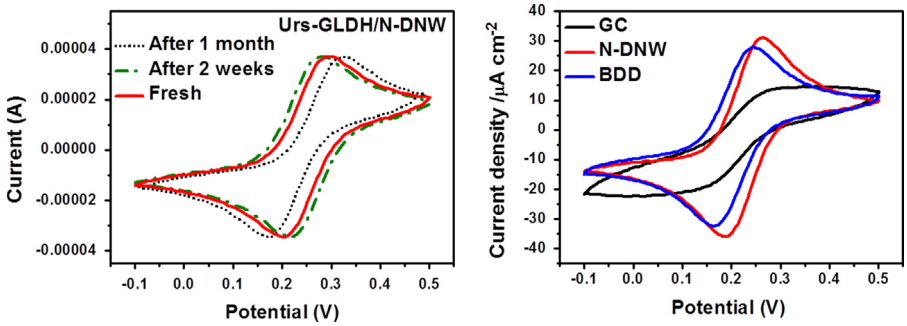

Fig. 5. (a) The stability of the Urs–GLDH/N-DNW bioelectrode (fresh, after 2 weeks and after 1 month) as a function of urea concentration in the presence of 30 μL of NADH and 70 μL of α-KG in PBS solution. (b) Cyclic voltammetry (CV) for Urs–GLDH immobilized N-DNW, BDD and GC electrode as a function of urea concentration in the presence of 30 μL of NADH and 70 μL of α –KG in PBS solution containing 0.5 M $[Fe(CN_6)]^{3-/4-}$ redox couples.

N-DNW electrode is wet-chemically cleaned (oxidation) by boiling in a mixture of H_2SO_4 and HNO_3 (3:1) at 200 °C for 2 h to remove graphite. Urs and GLDH are covalently attached to the oxidized N-DNW electrode by activating the COOH group of N-DNW using EDC as the coupling agent and NHS as activator. FTIR and XPS have represented its functionalized behavior. This Urs–GLDH/N-DNW has been successfully utilized in urea biosensor application employing an EC technique, which suggests its potential application in EC sensing and biosensing area. This Urs–GLDH/N-DNW biosensor shows linearity of 10–100 mg/dL, sensitivity of 6.18 μA/mg dL/cm^2, lower detection limit of 3.87 mg dL^{-1}, response time of >10 s and longtime stability. Thus, the sensor exhibited good performance in sensitivity, stability and reproducibility. Urs–GLDH/N-DNW also exhibited linear response when tested for different concentration of human urine in buffer solution (from 1:9 to 4:6). Urs–GLDH/N-DNW bioelectrode retained 80% of its initial enzyme activity for <1 month, when stored at 4–6 °C in a refrigerator. All these advantageous features can make the proposed biosensor applicable in medical, food or other areas.

Acknowledgments

The authors thank the National Science Council, Taiwan, for financial support under the contracts NSC98-2221-E-007-045-MY3 and NSC99-2119-M-032-003-MY2.

Appendix A. Supporting information

Supplementary data associated with this article can be found in the online version at http://dx.doi.org/10.1016/j.bios.2013.11.071.

References

Cabrera, C.R., Cunci, L., 2011. Electrochem. Solid-State Lett. 14, 17–19.
Danielsson, B., Harborn, U., Mecklenburg, M., Xie, B., 1994. Clin. Chem. 40, 2282–2287.
Danielsson, B., Nur, O., Willander, M., Usman Ali, S.M., 2009. IEEE Trans. Nanotechnol. 8, 678–683.
Danielsson, B., Nur, O., Willander, M., Usman Ali, S.M., 2010a. Sens. Actuators B: Chem. 145, 869–874.
Danielsson, B., Usman Ali, S.M., Nur, O., Willander, M., Brannmark, C., Stralfors, P., Englund, U., Elinder, F., Asif, M.H., 2010b. Biosens. Bioelectron. 25, 2205–2211.
Danielsson, B., Alvi, N.H., Ibupoto, Z., Nur, O., Willander, M., Usman Ali, S.M., 2011a. Sens. Actuators B 2, 241–247.
Danielsson, B., Asif, M.H., Fulati, A., Nur, O., Willander, M., Brannmark, C., Stralfors, P., Englund, U.H., Elinder, F., Usman Ali, S.M., 2011b. IEEE Trans. Nanotechnol. 10, 913–919.
Davidson, J.L., Kang, W.P., Raina, S., 2008. Diam. Relat. Mater. 17, 896–899.
Do, J.S., Luo, Y.C., 2004. Biosen. Bioelectron. 20, 15–23.
Dong, S., Chen, X., Qu, X., Jia, J., Xu, Z., 2004. Biosens. Bioelectron. 20, 579–584.
Durrant, J.R., Astuti, Y., Duriaux, F., Gratzel, M., Topoglidis, E., 2003. Langmuir 19, 6894–6900.
Fahys, B., Herlem, G., Lakard, S., Antoniou, A., Lakard, B., 2004. Biosens. Bioelectron. 19, 641–647.
Fujishima, A., Patel, K., Hashimoto, K., Tenne, R., 1993. J. Electroanal. Chem. 347, 409–415.
Gemeiner, P., Tkac, J., Sturdik, E., Vostiar, I., 2002. Bioelectrochemistry 56, 113–115.
Kaneto, K., Takashima, W., Rajesh, B.V., 2005. Biomaterials 26, 3683–3690.
Lin, I.N., Liu, C.C., Tai, N.H., Lee, C.Y., Fang, W., Chen, L.J., 2008. J. Phys. Chem. C 112, 3759–3765.
Lin, I.N., Joseph, P.T., Tai, N.H., Sankaran, K.J., 2010. Diam. Relat. Mater. 19, 927–931.
Lin, I.N., Horng, C.C., Chiang, H.Y., Chen, H.C., Cheng, H.F., 2011. J. Phys. Chem. C 115, 13894–13900.
Lin, I.N., Kurian, J., Chen, H.C., Dong, C.L., Lee, C.Y., Tai, N.H., Sankaran, K.J., 2012. J. Phys. D Appl. Phys. 45, 365303–365311.
Lin, I.N., Sankaran, K.J., Dong, C.L., Lee, C.Y., Tai, N.H., Shalini, J., 2013. Nanoscale 5, 1159–1167.
Malhotra, B.D., Kaushik, A., Ansari, A.A., Sumana, G., Solanki, P.R., 2008a. Appl. Phys. Lett. 93, 163903–163906.
Malhotra, B.D., Solanki, P.R., Ansari, A.A., 2008b. Appl. Phys. Lett. 92, 263901–263903.
Malhotra, B.D., Solanki, P.R., Ansari, A.A., Ahmad, S., Kaushik, A., 2008c. Electrochem. Commun. 10, 1364–1368.
Malhotra, B.D., Kaushik, A., Chavhan, P.M., Maheshwari, S.N., Solanki, P.R., 2009. Electrochem. Commun. 11, 2272–2277.
Pleskov, Y., Nyikos, L., Sakharova, A., 1992. Electrochim. Acta 37, 973–978.
Renault, N.J., Montoriol, J., Sant, W., Martelet, C., Soldatkin, A.P., 2003. Biosens. Bioelectron. 19, 131–135.
Rick, W., 1990. Klinische Chemie und MikroskopieSpringer-Verlag, Berlin, pp. 245–247.
Rosenthal, H.L., 1955. Anal. Chem. 27, 1980–1982.
Scarsbrook, G.A., Hammersberg, J., Johnannson, E., Wilkstrom, T., Twitchen, D.J., Whitehead, A.J., Coe, S.E., Isberg, J., 2002. Science 297, 1670–1672.
Shin, H.S., Ansari, Z.A., Seo, H.K., Kim, G.S., Kim, Y.S., Khang, G., Ansari, S.G., 2008. Sens. Actuators B 132, 265–271.
Staryga, E., Wrzyszczynski, A., Paprocki, K., Szreiber, M., Uniszkiewicz, C., Torz-Piotrowska, R., 2009. J. Achiev. Mater. Manuf. Eng. 37, 486–491.
Swain, G.M., Wang, S., 2007. J. Phys. Chem. C 111, 3986–3995.
Swain, G.M., Witek, M.A., Sonthalia, p., Show, Y., 2003. Chem. Mater. 15, 879–888.
Swain, G.M., Show, Y., Wang, S., Stotter, J., 2005. Chem. Mater. 17, 4880–4888.
Szunerits, S., Denoyelle, A., Boukherroub, R., Actis, P., 2008. Electrochem. Commun. 10, 402–406.
Walcarius, A., Reybier, K., Marrakchi, M., Jaffrezic-Renault, N., Martelet, C., Kherrat, R., Hamlaoui, M.L., 2002. Anal. Chim. Acta 466, 39–45.
Wightman, R.M., Venton, B.J., 2003. Anal. Chem. 75, 414A–421A.
Wilson, M.S., 2005. Anal. Chem. 77, 1496–1502.
Yu, J., Ju, H., 2002. Anal. Chem. 74, 3579–3583.
Yu, R., Liu, Y., Yang, H., Yang, Y., Shen, G., Liu, Z., 2005. Electroanalysis 17, 1065–1070.
Zhi, J.F., Rao, T.N., Einaga, Y., Tian, R.H., 2006. Chem. Mater. 18, 939–945.